GEOPHYSICS, VOL. 84, NO. 6 (NOVEMBER-DECEMBER 2019); P. 1–9, 14 FIGS.
10.1190/GEO2019-0088.1

Relationships between the anisotropy parameters for transversely isotropic mudrocks

Fuyong Yan[1], Lev Vernik[2], and De-Hua Han[1]

ABSTRACT

Studying the empirical relations between seismic anisotropy parameters is important for the simplification and practical applications of seismic anisotropy. The elastic properties of mudrocks are often described by transverse isotropy. Knowing the elastic properties in the vertical and horizontal directions, a sole oblique anisotropy parameter determines the pattern of variation of the elastic properties of a transversely isotropic (TI) medium in all of the other directions. The oblique seismic anisotropy parameter δ, which determines seismic reflection moveout behavior, is important in anisotropic seismic data processing and interpretation. Compared to the other anisotropy parameters, the oblique anisotropy parameter is more sensitive to the measurement error. Although, theoretically, only one oblique velocity is needed to determine the oblique anisotropy parameter, the uncertainty can be greatly reduced if multiple oblique velocities in different directions are measured. If a mudrock is not a perfect TI medium but it is expediently treated as one, then multiple oblique velocity measurements in different directions should lead to a more representative approximation of δ or c_{13} because the directional bias can be reduced. Based on a data quality analysis of the laboratory seismic anisotropy measurement data from the literature, we found that there are strong correlations between the oblique anisotropy parameter and the principal anisotropy parameters when data points of more uncertainty are excluded. Examples of potential applications of these empirical relations are discussed.

INTRODUCTION

Shales or mudstones account for most of the bulk volume of sedimentary rocks and are the primary factor of seismic anisotropy in seismic exploration (Schoenberg et al., 1996). Shales are traditionally treated as the organic source rocks and seals of the petroleum reservoir. They are becoming important petroleum reservoir rocks with the advancing techniques in directional drilling and hydraulic fracturing. Understanding the elastic properties of shales is of great consequence in petroleum exploration. The elastic properties of shales are often described by transverse isotropy (Johnston and Christensen, 1995; Vernik and Liu, 1997; Jakobsen and Johansen, 2000; Wang, 2002; Sone, 2012). The elastic properties of a transversely isotropic (TI) medium are defined by five independent parameters. Relative to isotropic media whose elastic properties are determined by two independent parameters, including extra anisotropy parameter brings up great challenges in seismic data processing and interpretation. For isotropic rocks, although the elastic properties are defined by only two theoretically independent parameters (V_P and V_S), there are often strong correlations between them for the same type of sedimentary rocks (Castagna et al., 1985). These correlations are critical for the successful application of amplitude variation with offset interpretation techniques. With more unknown parameters in anisotropic seismic data processing and interpretation, finding the relationships between the anisotropy parameters could be vital for practical applications of seismic anisotropy.

It is well-known that the P-wave velocity or modulus has a strong correlation with the S-wave velocity or modulus in either the vertical or horizontal directions for mudstones (Castagna et al., 1985; Horne, 2013). Using velocity anisotropy data of various sources (primarily laboratory core data, and other data from cross-dipole sonic, crosswell, and walkaway vertical seismic profile), Horne (2013) statistically studies the relationships among the anisotropic parameters. It is found that c_{11} and c_{66} and c_{33} and c_{44} have good

Manuscript received by the Editor 8 February 2019; revised manuscript received 19 July 2019; published ahead of production 29 August 2019.
[1]University of Houston, Department of Earth and Atmospheric Sciences, Houston, Texas, USA. E-mail: yanfyon@yahoo.com (corresponding author); dhan@uh.edu.
[2]Ikon Science, Houston, Texas, USA. E-mail: verniklev@gmail.com.

correlations. The relationships between c_{13} and the other elastic constants are not clear.

The oblique stiffness c_{13} determines the pattern of variation of the elastic properties from the vertical direction to the horizontal direction for a TI medium. Laboratory estimation of c_{13} requires at least one oblique velocity measurement. This oblique velocity can be a quasi-P-wave or a quasi-S-wave. A quasi-P-wave is commonly used because it is usually the first-arrived signal and is favorable for accurate traveltime picking. The propagating direction of a quasi-P-wave is different with the direction of the particle motion. They are related to two velocity vectors, phase velocity and group velocity. They are different in direction and magnitude. Failure to understand the differences and the special requirements on the measurement setup may introduce significant uncertainty in estimating c_{13} and δ (Yan et al., 2016, 2018). In this study, we primarily study the relationship between the elastic moduli and combinations thereof measured in the oblique and principal directions with respect of the symmetry elements of a TI medium based on the analysis of the laboratory anisotropy measurement data from the literature.

THEORY

The elastic properties of a TI medium are specified by five independent elastic constants. Using the Voigt notation, the elastic stiffness tensor of a TI medium with a symmetry axis aligned in the x_3-direction is expressed by

$$\mathbf{C} = \begin{pmatrix} c_{11} & c_{11}-2c_{66} & c_{13} & 0 & 0 & 0 \\ c_{11}-2c_{66} & c_{11} & c_{13} & 0 & 0 & 0 \\ c_{13} & c_{13} & c_{33} & 0 & 0 & 0 \\ 0 & 0 & 0 & c_{44} & 0 & 0 \\ 0 & 0 & 0 & 0 & c_{44} & 0 \\ 0 & 0 & 0 & 0 & 0 & c_{66} \end{pmatrix}. \tag{1}$$

The concept of Poisson's ratio for an isotropic medium can be straightforwardly extended to a TI medium using Hooke's law (King, 1964; Yan et al., 2016). Their relations with the TI elastic constants are as follows:

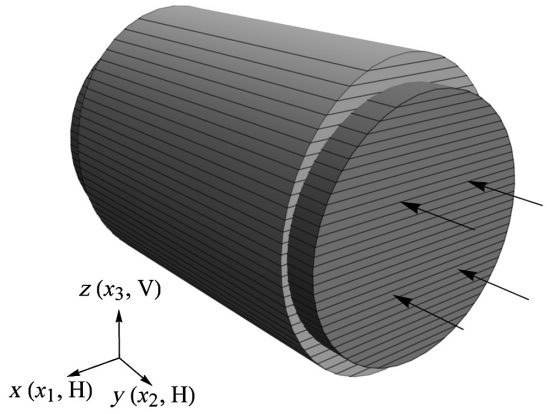

Figure 1. Diagram of deformation of a horizontal core plug under uniform axial compressional stress and the coordinate systems.

$$E_V = \frac{c_{33}(c_{11}-c_{66}) - c_{13}^2}{c_{11}-c_{66}} \quad (= E_3), \tag{2}$$

$$E_H = \frac{4c_{66}(c_{33}(c_{11}-c_{66}) - c_{13}^2)}{c_{11}c_{33}-c_{13}^2} \quad (= E_1 = E_2), \tag{3}$$

$$\nu_V = \frac{c_{13}}{2(c_{11}-c_{66})} \quad (= \nu_{31} = \nu_{32}), \tag{4}$$

$$\nu_{HV} = \frac{2c_{13}c_{66}}{c_{11}c_{33}-c_{13}^2} \quad (= \nu_{13} = \nu_{23}), \tag{5}$$

$$\nu_{HH} = \frac{c_{33}(c_{11}-2c_{66}) - c_{13}^2}{c_{11}c_{33}-c_{13}^2} \quad (= \nu_{12} = \nu_{21}), \tag{6}$$

where E_V and E_H are the Young's modulus in the vertical and horizontal directions, respectively. There are three principal Poisson's ratios: ν_V, ν_{HV}, and ν_{HH}. The coordinate system used for the notation is shown in Figure 1.

The Thomsen parameters are more convenient and commonly used in exploration geophysics, and they are defined as (Thomsen, 1986)

$$\varepsilon = \frac{c_{11}-c_{33}}{2c_{33}}, \tag{7}$$

$$\gamma = \frac{c_{66}-c_{44}}{2c_{44}}, \tag{8}$$

$$\delta = \frac{(c_{13}+c_{44})^2 - (c_{33}-c_{44})^2}{2c_{33}(c_{33}-c_{44})}. \tag{9}$$

Figure 1 also shows the schematic deformation of a horizontal plug of a TI medium under uniform axial compression. The deformation in the radial directions of the cylindrical sample will not be uniform due to elastic anisotropy, and two principal Poisson's ratios (ν_{HH} and ν_{HV}) can be measured from the compressional testing. Based on the static mechanical measurements and physical intuition, Yan et al. (2016) argue that a practical relationship exists between these two principal Poisson's ratios for hydrocarbon source rocks:

$$0 < \nu_{HH} < \nu_{HV}. \tag{10}$$

For the dynamic properties, if the wavelength is much greater than the scale of the heterogeneity, the relation should still hold. Under the assumption in equation 10 and using the definitions of Poisson's ratios in equations 5 and 6, Yan et al. (2016) show that c_{13} is practically constrained by c_{11}, c_{33}, and c_{66} for TI mudrocks:

$$c_{13}^{-} < c_{33} < c_{13}^{+}, \tag{11}$$

where $c_{13}^{-}=\sqrt{c_{33}(c_{11}-2c_{66})+c_{66}^2}-c_{66}$ and $c_{13}^{+}=\sqrt{c_{33}(c_{11}-2c_{66})}$.

Sarout (2017) brings up an antiexample for the above physical constraints using Postma's two-layer model (Postma, 1955). The real mudrocks may be more complicated than a model of two isotropic layers and the theoretical assumption of perfect bonding might not be satisfied. Chichinina and Vernik (2018) agree upon the lower constraint that by coincidence equals to the constraint of the linear-slip model (Schoenberg, 1980); however, they also suggest a tighter upper bound based on Postma's model:

$$c_{13\,\max} = \sqrt{(c_{11}-c_{44})(c_{33}-c_{44})}-c_{44}. \tag{12}$$

In terms of the Thomsen parameters, they showed that this tighter upper bound on c_{13} is equivalent to the following simple equality:

$$\delta_{\max} = \varepsilon. \tag{13}$$

The modified constraints comply very well with the data carefully complied by Vernik (2016). Equation 13 may be quite useful due to its extreme simplicity. The tighter upper constraint in equation 12 is based on a periodical, perfectly bound two-layer model consisting of two isotropic materials. It may be generally applicable to organic mudrocks, but it should be considered quite heuristic (Chichinina and Vernik, 2018). By default, the more general physical constraints by Yan et al. (2016) will be used in this study.

LABORATORY VELOCITY ANISOTROPY MEASUREMENT

The five stiffnesses defining a TI medium can be determined by a minimum of five velocity measurements. Usually, the four principal stiffnesses are measured in the directions along or perpendicular to the TI symmetry,

$$c_{11} = \rho V_{\mathrm{P90}}^2, \tag{14}$$

$$c_{33} = \rho V_{\mathrm{P0}}^2, \tag{15}$$

$$c_{44} = \rho V_{\mathrm{SH0}}^2 = \rho V_{\mathrm{SV0}}^2 = \rho V_{\mathrm{SV90}}^2, \tag{16}$$

$$c_{66} = \rho V_{\mathrm{SH90}}^2, \tag{17}$$

where the subscripts P, SV, and SH denote the three wave modes in an anisotropic medium, respectively. To determine c_{13}, at least one oblique velocity must be measured in an oblique direction relative to the symmetry elements of a TI medium. The oblique velocity can be quasi-P-wave or SV-wave, but usually quasi-P-wave is preferred because there are often converted wave signals before the SV-wave signal. If a quasi-P-wave phase velocity is measured, c_{13} can be calculated using (Yan et al., 2012)

$$c_{13} = \frac{2}{\sin 2\theta}\sqrt{(\rho V_{\mathrm{P}\theta}^2 - c_{11}\sin^2\theta - c_{44}\cos^2\theta)(\rho V_{\mathrm{P}\theta}^2 - c_{33}\cos^2\theta - c_{44}\sin^2\theta)} - c_{44}, \tag{18}$$

where θ denotes the phase velocity or phase angle. If only one oblique velocity is measured, it is usually approximately 45°. If an oblique group velocity is measured, c_{13} can be numerically inverted from the combination of equation 18 and the following relations (Byun, 1984):

$$\mathrm{Tan}(\varphi-\theta) = \frac{1}{V_\theta}\frac{\mathrm{d}V_\theta}{\mathrm{d}\theta}, \tag{19}$$

$$V_\theta = V_\varphi \cos(\varphi-\theta), \tag{20}$$

where V can be either P-, SV-, or SH-wave velocity and φ is the group angle and denotes the group velocity when it is used as a subscript.

CORRELATIONS BETWEEN THE ANISOTROPY PARAMETERS

Although the five stiffnesses defining a TI medium are theoretically independent, for a specified type of TI medium, such as the organic mudrocks, there can be strong relationships among the five stiffnesses. The well-known mudrock line is actually an empirical linear relation between the vertical P- and S-wave velocities (Castagna et al., 1985). Figure 2 shows the correlations between the principal stiffnesses using laboratory anisotropy measurement data from the literature. The correlation between c_{11} and c_{66} is stronger than that between c_{33} and c_{44}. The correlation is further improved when all of the principal stiffnesses are included. If only one of the vertical or horizontal velocities is unavailable, it could be reliably predicted from the other principal velocities.

Figure 3 shows the correlation between c_{13} and the principal stiffnesses. It is obvious that c_{13} is correlated with the other stiffnesses, but the correlation is weaker than those correlations between the principal stiffnesses shown in Figure 2 even though more regression variables are included. In anisotropic seismic data processing and interpretation, the Thomsen parameters are more convenient for application than are the stiffness parameters. Corresponding to c_{13}, δ is the sole Thomsen parameter determining how the seismic velocities transit from the vertical direction to the horizontal direction. Figure 4 shows the correlation between δ and the other Thomsen parameters. Here, α and β are the vertical P- and S-wave velocities, respectively. The correlation is weak with a correlation coefficient of 0.21. If we have little confidence in the empirical relation, it might not be useful as a constraint for inverting anisotropy parameters from sonic or seismic data. As we discussed earlier, the laboratory measurements of the principal anisotropy parameters are straightforward, but there is significant uncertainty in estimating the oblique anisotropy parameter δ. The deterioration of the correlation between the oblique anisotropy parameter and the other anisotropy parameters could be caused by the uncertainty related to the measurement in the oblique direction.

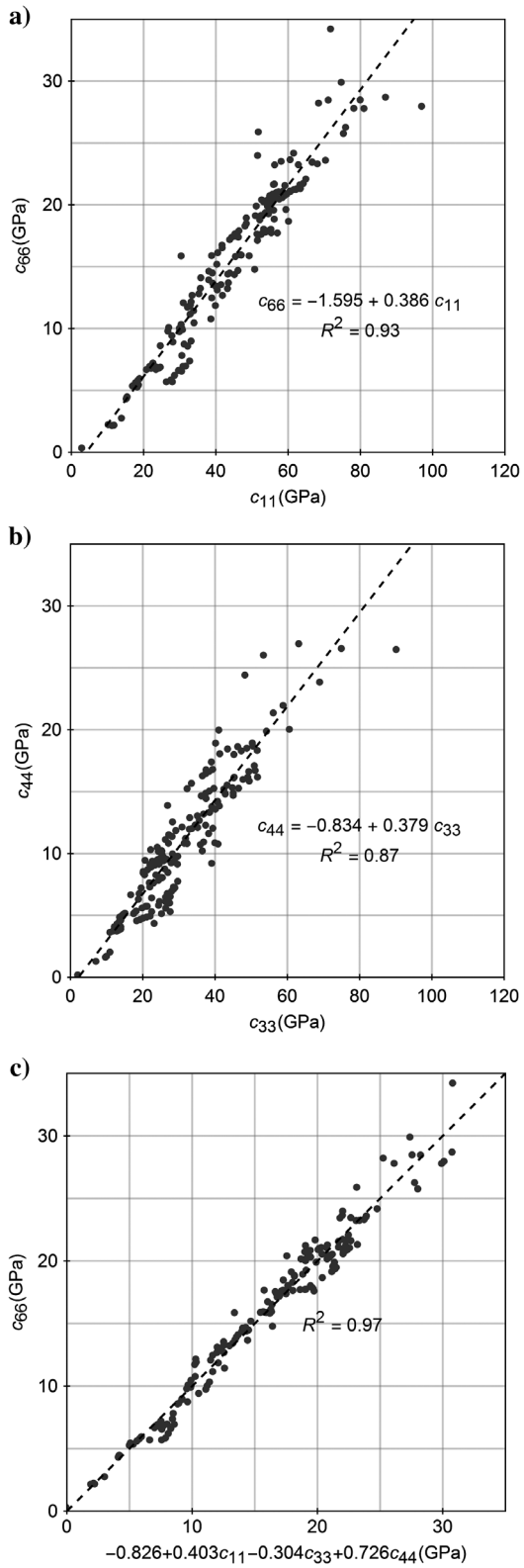

Figure 2. Relationships between the principal stiffnesses. (a) The correlation between c_{11} and c_{66}, (b) the correlation between c_{33} and c_{44}, and (c) the correlation between c_{66} and c_{11} and c_{33} and c_{44}. The data come from Thomsen (1986), Johnston and Christensen (1995), Jakobsen and Johansen (2000), Wang (2002), Sone (2012), and Vernik (2016).

UNCERTAINTY IN LABORATORY MEASUREMENT OF c_{13} OR δ

There are various laboratory measurement setups for determining all five TI anisotropy parameters. Most commonly, the measurement is based on three core plugs (Vernik and Nur, 1992): one vertical plug, one horizontal plug, and one 45° plug. It can also be based on a single vertical plug (Jakobsen and Johansen, 2000), a single horizontal plug (Wang, 2002), and more than three plugs (Johnston and Christensen, 1995; Sone, 2012). The different setups may have different advantages with respect to the measurement efficiency, accuracy, and ability to simulate in situ stress conditions. Here, we are primarily concerned with the measurement accuracy of the oblique anisotropy parameter, c_{13} or δ.

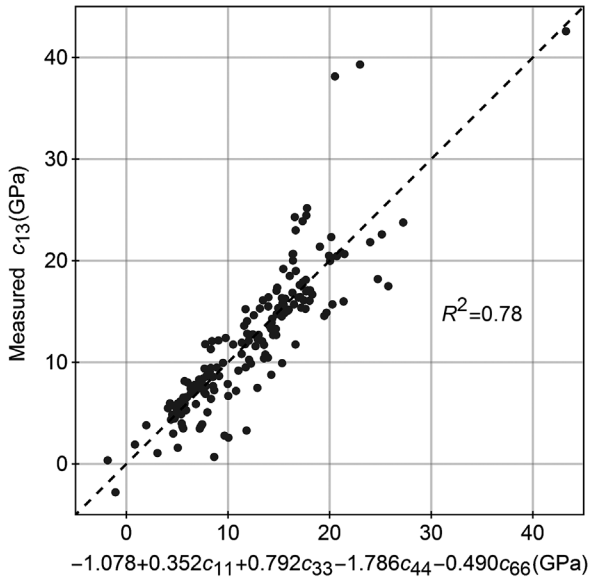

Figure 3. Correlation between c_{13} and the other stiffnesses. The data sources are the same as those in Figure 2.

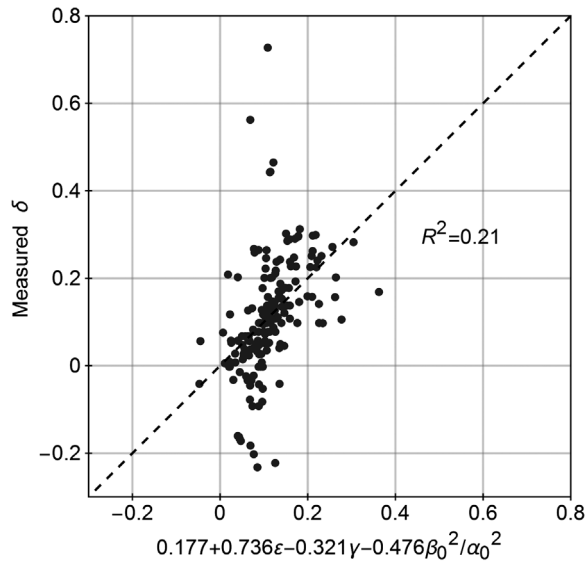

Figure 4. Correlation between δ and the other Thomsen parameters. The same data sources as in Figure 3 are used.

Based on the measurement setup used by Vernik and Nur (1992), and Dellinger and Vernik (1994) discuss the confusion about the group or phase velocity measured on a 45° core plug. They conclude that Vernik and Nur (1992) generally measure the 45° P-wave phase velocity, but there might be a slight underestimation. Yan et al. (2018) study the effect of geometric relation between the piezoelectric transducer and the core sample on the oblique velocity measurement by modeling the wavefront propagation on the 45° core plug and the horizontal core plug. Yan et al. (2018) also discuss various factors that may affect the accurate estimation of c_{13} or δ for the various measurement setups. It is critical that a genuine phase velocity or group velocity is measured. The geometric configuration of the piezoelectric transducer and its relative dimensions to those of the sample can have a significant effect on the accuracy of the oblique velocity measurement. Although, theoretically, only one oblique velocity is sufficient to determine c_{13} or δ with the other principal parameters being known, the accuracy should be greatly improved if multiple oblique velocities are measured at different directions. Quite often, the mudrocks might not be a perfect TI medium. Instead, they are approximated as a TI medium for the convenience of applications. Under such circumstances, more measurements from different directions should be made so that the approximation is not biased by the measurement result from a specified direction.

Figure 5 shows a statistical description of the relation between the measured c_{13} and its physical constraints (equation 11) using the data collected from the literature. The data collected by Thomsen (1986) are from various sources; only data points with anisotropy stronger than the measurement uncertainty ($\varepsilon > 0.03$ and $\gamma > 0.03$) are included. Wang's data are corrected for mistaking the group velocity for the phase velocity in the oblique direction and under the assumption that a genuine 45° group velocity is measured (Yan et al., 2016). If there is a pressure-dependent measurement, no more than three data points are used for the same sample to prevent the overweighting effect of this sample. For the data sets by Johnston and Christensen (1995) and Sone (2012), the estimation of c_{13} is based on the least-squares regression of multiple oblique P-wave phase velocities, and in the measurement setup designing, the dimension of the piezoelectric transducer relative to the sample is sufficiently large to ensure that the genuine phase velocity is measured. Therefore, the data sets by Johnston and Christensen (1995) and Sone (2012) have less uncertainty in the estimation of c_{13} than the other data sets, and they are all within the physical constraints proposed by Yan et al. (2016). The data set by Vernik (2016) is based on strict quality checking of the previous measurements (Vernik and Nur, 1992; Vernik and Liu, 1997), and the data quality is relatively good, although only one oblique P-wave velocity is measured for the determination of c_{13}.

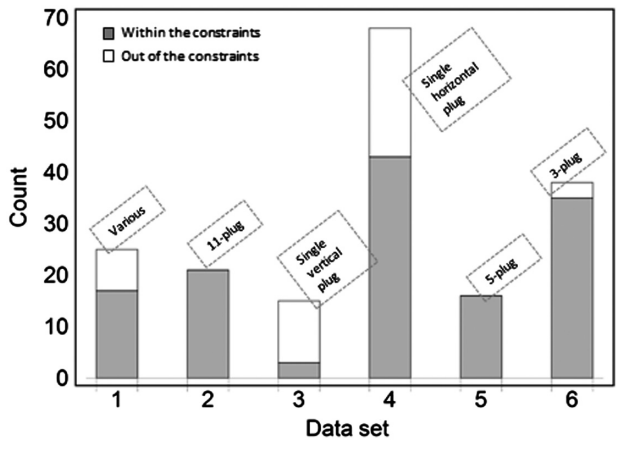

Figure 5. A statistical description of the relation between c_{13} and its physical constraints. The data sources are (1) Thomsen (1986), (2) Johnston and Christensen (1995), (3) Jakobsen and Johansen (2000), (4) Wang (2002), (5) Sone (2012), and (6) Vernik (2016).

If the tighter upper bound suggested by Chichinina and Vernik (2018) is used to plot Figure 5, the results are similar. The data points from the data sets by Johnston and Christensen (1995) and Sone (2012) all lay within the bounds, and there are more data points out of the tighter bounds for the other data sets. Therefore, the physical constraints on c_{13} by Yan et al. (2016) and Chichinina and Vernik (2018) can be used to check the data quality of laboratory seismic anisotropy measurements on mudrocks.

IMPROVED CORRELATIONS USING DATA SETS OF BETTER QUALITY CONTROL

From the above discussion, the data points with c_{13} out of the physical constraints may have significant measurement uncertainty. The correlation between the oblique and the principal anisotropy parameters will deteriorate if too many data points with substandard quality are included. In Figure 6, the correlation is based on data points with c_{13} located in the physical constraints, and the data points with c_{13} out of the constraints are plotted along for comparison. Compared with Figure 4, the correlation is obviously improved by using only the data points with c_{13} in the constraints, and the data points with c_{13} out of the constraints are mostly outliers. Similarly, Figure 7 shows the correlation between δ and the other principal Thomsen parameters. Compared with Figure 5, the correlation is significantly improved by using only the data points with c_{13} in the constraints, and the outliers are mostly the data points with c_{13} out of the constraints. Therefore, the significant uncertainty related to the measurement in the oblique direction can substantially deterio-

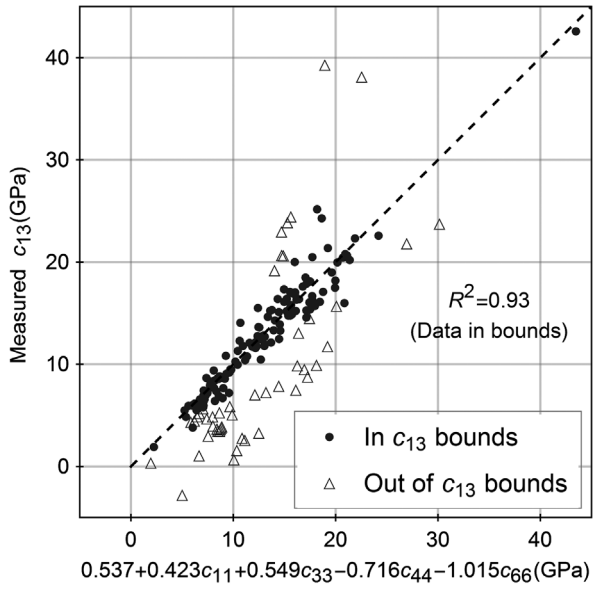

Figure 6. Correlation between c_{13} and the other principal stiffnesses using data points within the practical bounds of c_{13}.

rate the correlation between the oblique and the principal anisotropy parameters.

For the data sets by Johnston and Christensen (1995) and Sone (2012), multiple oblique P-wave velocities are measured to reduce the directional bias in estimating c_{13} and δ. The correlations should be further improved if only data points from these data sets are i ncluded. Indeed, as shown in Figures 8 and 9, the correlations between the oblique anisotropy parameters and the principal anisotropy parameters are noticeably improved over those shown in Figures 6 and 7. It should be noted that the samples used by Sone (2012) are from different reservoirs in the North America, including the Barnett, Haynesville, Eagle Ford, and Fort St. John Formations. The correlations based on data sets 2 and 5 may still be representative of the anisotropic properties of organic mudrocks to a certain degree. It would be desirable if more high-quality anisotropy measurement data like those by Johnston and Christensen (1995) and Sone (2012) would be available in the future. There are always upscaling issues when we apply the laboratory core measurement results to the field data. The empirical relations should be applied with caution because an empirical relation based on the measurement of core samples from one reservoir is not necessarily applicable to another reservoir. It is always preferred that local calibration can be conducted.

POTENTIAL APPLICATIONS OF THE CORRELATIONS

Hydraulic fracturing is a critical technique for the development of unconventional hydrocarbon resources. An effective fracturing of the mudrocks needs information of the mechanical properties of the mudrocks and the in situ stress. The organic mudrocks are often approximated as a TI medium, whose mechanical properties are described by two principal Young's moduli and three principal Poisson's ratios. These mechanical anisotropy parameters are defined in equations 2–6, and they are basic inputs for predicting the in situ stress in a TI medium (Higgins et al., 2008). From equations 2 and 6, four stiffnesses, c_{11}, c_{33}, c_{66}, and c_{13}, are needed to define the five mechanical anisotropy parameters. In the field applications, determining c_{13} may be more challenging than in the laboratory. If c_{11}, c_{33}, and c_{66} are available, for example, from the acoustic logging data in the vertical and horizontal sections of a formation, the c_{13} can be estimated from correlation established from the laboratory measurements, and then Young's moduli and Poisson's ratios can be estimated. Here, we assume that the differences between the static and dynamic properties of the subsurface organic mudrocks are negligible when they are under the in situ conditions (Yan et al., 2017).

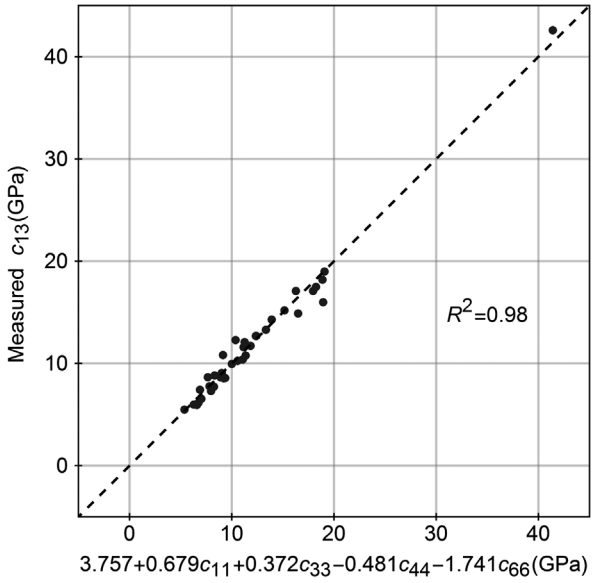

Figure 8. Correlation between c_{13} and the other stiffnesses using data sets 2 and 5 shown in Figure 5.

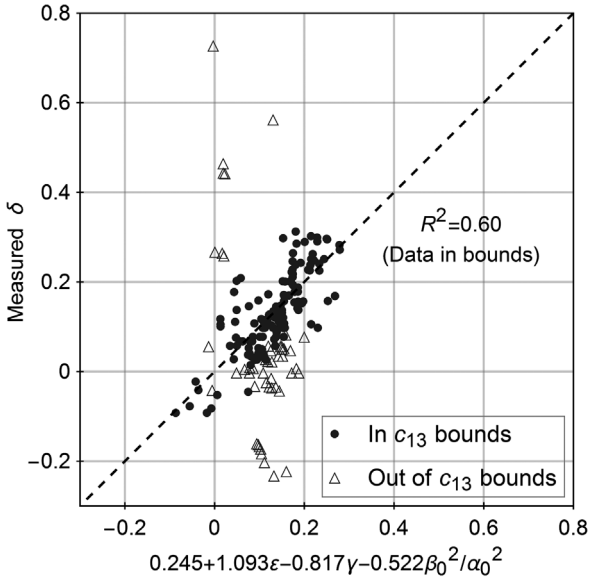

Figure 7. Correlation between δ and the other Thomsen parameters using data points with c_{13} lying within the physical constraints. The same data sources as Figure 3 are used.

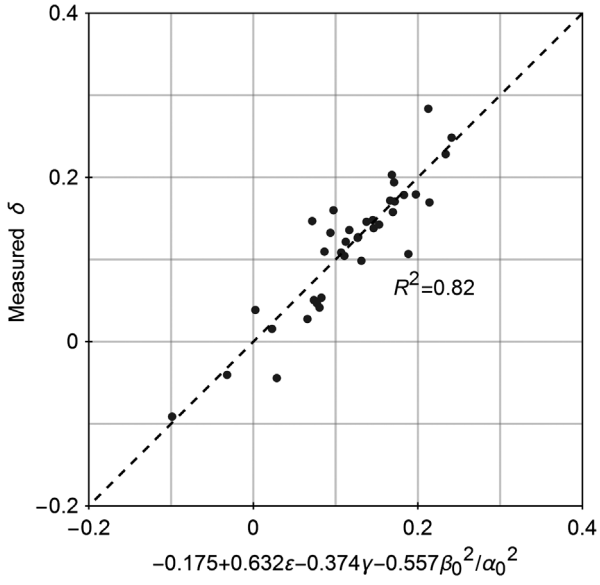

Figure 9. Correlation between δ and the other Thomsen parameters using data sets 2 and 5 shown in Figure 5.

In Figure 10, c_{13} is correlated with c_{11}, c_{33}, and c_{66} using data sets 2 and 5 shown in Figure 5. Compared with Figure 8, the correlation is not obviously weakened when c_{44} is not included. Figures 11 and 12 show the predicted Young's moduli and Poisson's ratio, respectively, using c_{13} estimated from the empirical relation shown in Figure 10. The standard error for the correlation shown in Figure 10 is 1.39 GPa, and the standard error for the correlation shown in Figure 11 is 0.21 GPa. The regression coefficient R^2 is 0.900 for the prediction of the Poisson's ratios, and it is 0.998 for the prediction of the Young's moduli. Therefore, the prediction of the Poisson's ratios is more sensitive to the error in estimating c_{13} than the prediction of the Young's moduli, but the result is still satisfactory. Strictly speaking, the estimated Young's moduli and Poisson's ratios in Figures 11 and 12 are not predictions because the empirical relations are set up on the same data set, but they show a potential application of the empirical relation between c_{13} and the other principal stiffnesses.

The prerequisite for practical application of seismic anisotropy is that the anisotropy parameters can be reliably estimated. The synthetic study by Yan and Han (2018) demonstrated that there are great challenges in reliable estimation of the anisotropy parameters for a layer-cake model even when the vertical properties are known, and the noise level is lower than the common field seismic data. To

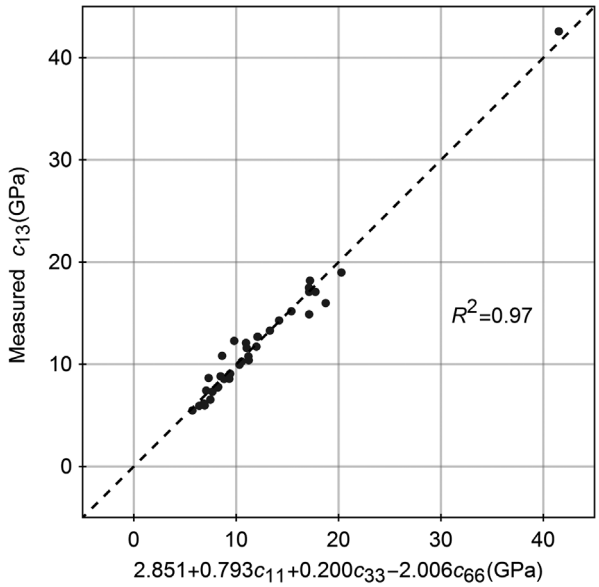

Figure 10. Correlation of c_{13} with c_{11}, c_{33}, and c_{66} using data sets 2 and 5 shown in Figure 5.

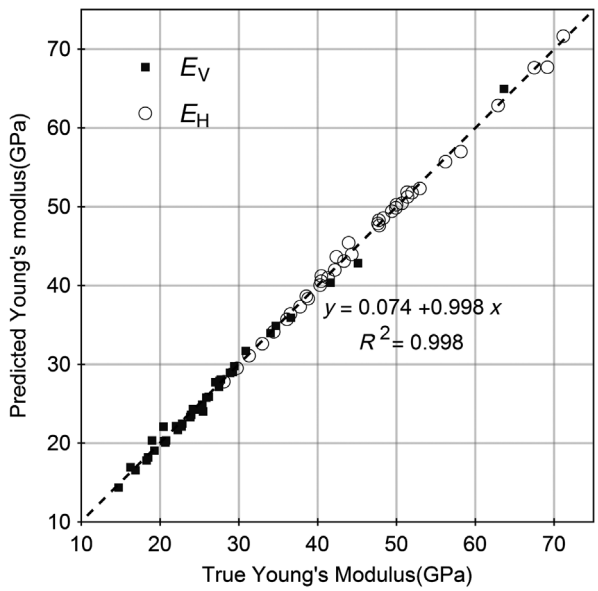

Figure 11. Estimated Young's moduli using c_{13} calculated from the empirical relation shown in Figure 10.

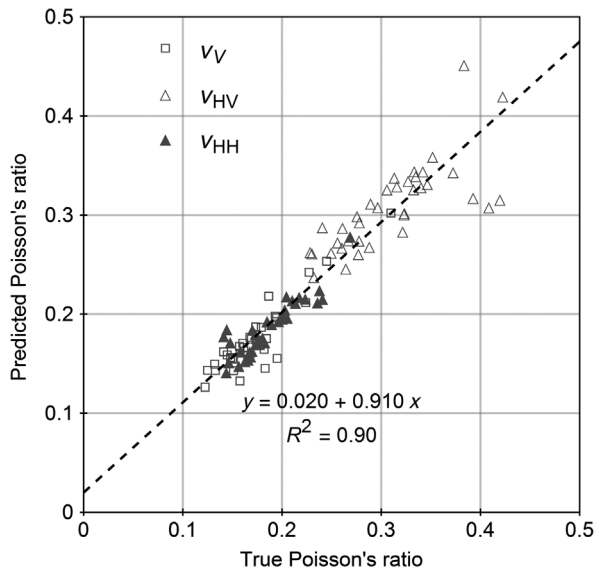

Figure 12. Estimated Poisson's ratios using c_{13} calculated from the empirical relation shown in Figure 10.

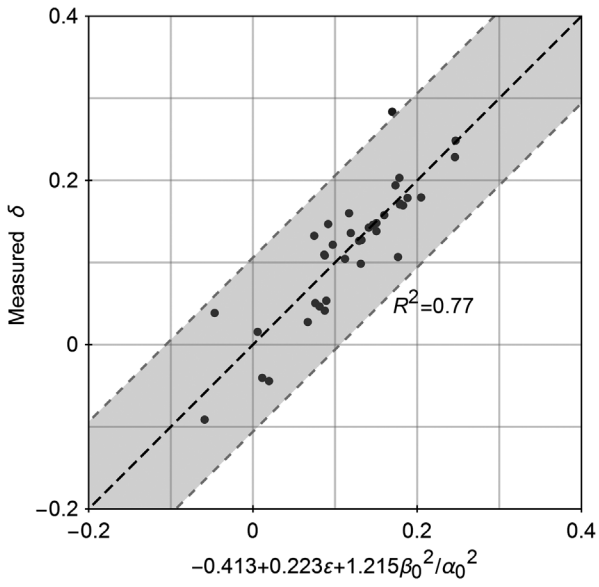

Figure 13. Correlation of δ with ε and the ratio of β_0 to α_0 using data sets 2 and 5 shown in Figure 5. The gray area marks the region within the 95% confidence level.

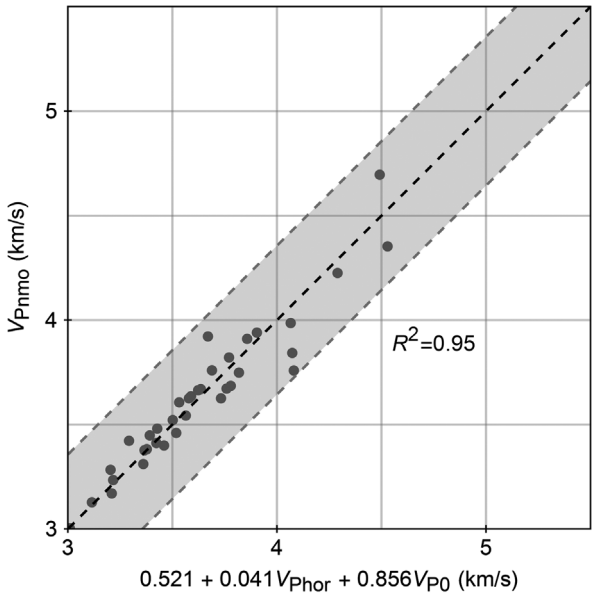

Figure 14. Correlation of V_{Pnmo} with V_{Phor} and V_{P0} data sets 2 and 5 shown in Figure 5. The gray area marks the region within the 95% confidence level.

decrease the uncertainties in estimating anisotropy parameters, one possible way is to use the empirical relationships observed in laboratory studies to constrain the inverted anisotropy parameters. It is assumed that the laboratory-measured parameters are representative of the reservoir formations. Figures 13 and 14 show two forms of correlations that might be useful for constraining the inverted anisotropy parameters. A confidence level is given so that we should seek the to-be-inverted seismic anisotropy parameters in the confidence area. In consideration of practical applications, Thomsen parameter γ is not included in the relationship because it is primarily related to the pure S-wave, and in a sense, it is independent of ε and δ. The correlation shown in Figure 13 may be more useful than the relation shown in Figure 9. The correlation is not significantly weakened by the exclusion of γ. If the vertical V_S-V_P ratio is known, then the empirical relation with a certain confidence level as shown in Figure 13 can be used to constrain the inverted Thomsen parameters ε and δ.

From the quadratic P-wave reflection moveout equation by Tsvankin (2012), the P-wave reflectivity is sufficiently described by three anisotropy parameters, V_{P0}, V_{Pnmo}, and V_{Phor}, with

$$V_{Pnmo} = V_{P0}\sqrt{1+2\delta}, \tag{21}$$

$$V_{Phor} = V_{P0}\sqrt{1+2\varepsilon}, \tag{22}$$

where V_{Pnmo} is the normal moveout P-wave velocity and V_{Phor} is the horizontal P-wave velocity that is also denoted as V_{P90}. The empirical relation with a 95% confidence level shown in Figure 14 can be applied as effective constraints to improve the accuracy in estimating the anisotropy parameters using the procedure by Tsvankin (2012).

CONCLUSION

For organic mudrocks with transverse isotropy, there exist strong correlations between the anisotropy parameters. The strong correlation between the oblique anisotropy parameter and the principal anisotropy parameters can be concealed due to uncertainty in the estimation of c_{13} or δ. The most accurate results are typically obtained when multiple oblique velocities are measured on multiple core plugs of different orientations. The strong correlations might be useful in applications of geomechanics and seismic anisotropy on shale formations.

DATA AND MATERIALS AVAILABILITY

Data associated with this research are available and can be obtained by contacting the corresponding author.

ACKNOWLEDGMENTS

We thank I. Bayuk and two anonymous reviewers for the valuable comments and suggestions that greatly improved this paper.

REFERENCES

Byun, B. S., 1984, Seismic parameters for transversely isotropic media: Geophysics, **49**, 1908–1914, doi: 10.1190/1.1441603.
Castagna, J. P., B. L. Batzle, and R. L. Eastwood, 1985, Relationships between compressional-wave and shear-wave velocities in clastic silicate rocks: Geophysics, **50**, 571–581, doi: 10.1190/1.1441933.
Chichinina, T., and L. Vernik, 2018, Physical bounds on c_{13} and δ for organic mudrocks: Geophysics, **83**, no. 5, A75–A79, doi: 10.1190/geo2018-0035.1.
Dellinger, J., and L. Vernik, 1994, Do traveltimes in pulse-transmission experiments yield anisotropic group or phase velocities: Geophysics, **59**, 1774–1779, doi: 10.1190/1.1443564.
Higgins, S., S. Goodwin, A. Donald, T. Bratton, and G. Gracy, 2008, Anisotropic stress models improve completion design in the Baxter Shale: Annual Technical Conference and Exhibition, doi: 10.2118/115736-MS.
Horne, S. A., 2013, A statistical review of mudstone elastic anisotropy: Geophysical Prospecting, **61**, 817–826, doi: 10.1111/1365-2478.12036.
Jakobsen, M., and T. A. Johansen, 2000, Anisotropic approximations for mudrocks: A seismic laboratory study: Geophysics, **65**, 1711–1725, doi: 10.1190/1.1444856.
Johnston, J. E., and N. I. Christensen, 1995, Seismic anisotropy of shales: Journal of Geophysical Research, **100**, 5591–6003.
King, M. S., 1964, Wave velocities and dynamic elastic moduli of sedimentary rocks: Ph.D. thesis, University of California.
Postma, G. W., 1955, Wave propagation in a stratified medium: Geophysics, **20**, 780–806, doi: 10.1190/1.1438187.
Sarout, J., 2017, Comment on "Physical constraints on c_{13} and δ for transversely isotropic hydrocarbon source rocks" by F. Yan, D.-H. Han, and Q. Yao, Geophysical Prospecting, 57, 393–411: Geophysical Prospecting, **65**, 379–380, doi: 10.1111/1365-2478.12359.
Schoenberg, M., 1980, Elastic wave behavior across linear slip interfaces: Journal of Acoustical Society of America, **68**, 1516–1521, doi: 10.1121/1.385077.
Schoenberg, M., F. Muir, and C. Sayers, 1996, Introducing ANNIE: A simple three-parameters anisotropic velocity model: Journal of Seismic Exploration, **5**, 35–49.
Sone, H., 2012, Mechanical properties of shale gas reservoir rocks and its relation to in-situ stress variation observed in shale gas reservoirs: Ph.D. thesis, Stanford University.
Thomsen, L., 1986, Weak elastic anisotropy: Geophysics, **51**, 1954–1966, doi: 10.1190/1.1442051.
Tsvankin, I., 2012, Seismic signatures and analysis of reflection data in anisotropic media, 3rd ed.: SEG.
Vernik, L., 2016, Seismic petrophysics in quantitative interpretation, 2nd ed.: SEG, Investigations in geophysics 18.
Vernik, L., and X. Liu, 1997, Velocity anisotropy in shales: A petrophysical study: Geophysics, **62**, 521–532, doi: 10.1190/1.1444162.
Vernik, L., and A. Nur, 1992, Ultrasonic velocity and anisotropy of hydrocarbon source rocks: Geophysics, **57**, 727–735, doi: 10.1190/1.1443286.
Wang, Z., 2002, Seismic anisotropy in sedimentary rocks — Part 2: Laboratory data: Geophysics, **67**, 1423–1440, doi: 10.1190/1.1512743.

Yan, F., and D.-H. Han, 2018, Accuracy and sensitivity analysis on seismic anisotropy parameter estimation: Journal of Geophysics and Engineering, **15**, 539–553, doi: 10.1088/1742-2140/aa93b1.

Yan, F., D.-H. Han, and X.-L. Chen, 2018, Practical and robust experimental determination of c_{13} and Thomsen parameter δ: Geophysical Prospecting, **66**, 354–365, doi: 10.1111/1365-2478.12514.

Yan, F., D.-H. Han, X.-L. Chen, J. Ren, and Y. Wang, 2017, Comparison of dynamic and static bulk moduli of reservoir rocks: 87th Annual International Meeting, SEG, Expanded Abstracts, 3711–3715, doi: 10.1190/segam2017-17664075.1.

Yan, F., D.-H. Han, and Q. Yao, 2012, Oil shale anisotropy measurement and sensitivity analysis: 82nd Annual International Meeting, SEG, Expanded Abstracts, doi: 10.1190/segam2012-1106.1.

Yan, F., D.-H. Han, and Q. Yao, 2016, Physical constrains on c_{13} and δ for transversely isotropic hydrocarbon source rocks: Geophysical Prospecting, **64**, 1524–1536, doi: 10.1111/1365-2478.12265.